Evidence for d-Orbital Aromaticity in Sn- and Pb-Based Clusters: Is Sn_{12}^{2-} Aromatic?

De-Li Chen,[†] Wei Quan Tian,*[,†] Ji-Kang Feng,[†,‡] and Chia-Chung Sun[†]

State Key Laboratory of Theoretical and Computational Chemistry, Institute of Theoretical Chemistry, and College of Chemistry, Jilin University, Changchun 130023, China

Received: May 13, 2007

The electronic structures and stabilities of pure M_{12}^- and M_{12}^{2-} were systematically investigated within density functional theory. The nucleus-independent chemical shifts (NICSs) of I_h Sn_{12}^{2-} and Pb_{12}^{2-} are −5.0 and −20.7 ppm, respectively, based on B3LYP/aug-cc-pVDZ-PP predictions, whereas the NICS of Sn_{12}^{2-} is predicted to be 1.1 ppm by B3LYP/LanL2DZ. A startling conclusion is that the $NICS_{4d}$ of Sn_{12}^{2-} and $NICS_{5d}$ of Pb_{12}^{2-} are −5.0 and −7.5 ppm, respectively, suggesting the significant contribution of the inner d orbitals to the total NICS values. This provides the first quantitative evidence for the existence of "d-orbital aromaticity" in Sn- and Pb-based clusters with three-dimensional structures. The d orbitals also contribute to the total NICSs of the K-coordinated clusters. The NICS predictions suggest that larger basis sets including d-orbitals are needed to analyze the aromaticity of some main-group-metal-based clusters (e.g., Sn- and Pb-based clusters) to obtain accurate predictions.

1. Introduction

Recently, some studies on metal-atom- (A-) encapsulated $A@Pb_{12}$ clusters with large stabilities were reported.[1−11] The large stabilities of the $A@Pb_{12}$ clusters were mainly attributed to the stability of Pb_{12}^{2-} cluster, which not only exhibits good geometrical balance but also has extra stability with cage aromaticity.[8,10,11] The cage aromaticity was evaluated with nucleus-independent chemical shifts (NICSs),[12−14] which is considered as an efficient way to predict aromaticity. Their lighter congeners, $A@Sn_{12}$, were also reported to exhibit large stabilities.[6,15] In addition, Wang et al.[16] synthesized the closed-shell I_h Sn_{12}^{2-} in the form of KSn_{12}^- [$K^+(Sn_{12}^{2-})$] and suggested that the stannaspherene (Sn_{12}^{2-}) exhibits a large stability. However, in Chen et al.'s work,[8] the NICS of Sn_{12}^{2-} was predicted to be 2.5 ppm, indicating the nonaromatic character of Sn_{12}^{2-}, which cannot explain its large stability. Thus, the question is raised as to whether the stannaspherene (Sn_{12}^{2-}) with large stability actually exhibits nonaromatic character. These studies stimulated our investigation.

Some investigations[17−20] have provided quantitative evidence for the existence of "d-orbital aromaticity" in transition-metal- (Cu-, Ag-, and Au-) based clusters where the d orbitals comprise the valence shell. A question to be answered in this work is whether such d-orbital aromaticity also exists in main-group-metal-based clusters in which the d orbitals are viewed as a fully occupied semicore. To clarify these questions, detailed analyses of the contributions to the aromaticity of Sn_{12}^{2-} (as well as Pb_{12}^{2-}) were performed to provide quantitative descriptions of such contributions. We found that Sn_{12}^{2-} is slightly aromatic because of the determining contributions from the d orbitals and that the application of larger basis sets including d orbitals to such clusters is necessary for aromaticity predictions. We studied the aromaticity of the K-coordinated KM_{12}, KM_{12}^-, and K_2M_{12} clusters as well.

2. Computational Details

Becke's hybrid three-parameter exchange functional[21] with the LYP correlation functional[22] (B3LYP) as implemented in the Gaussian 03 package[23] was employed in the calculations. The 6-31G(d) basis set was used for K atoms, whereas the energy-adjusted small-core ([core]$4s^24p^64d^{10}5s^25p^2$ and [core]$5s^25p^65d^{10}6s^26p^2$ for Sn and Pb, respectively.) pseudopotentials (PPs) were used for Sn and Pb atoms, labeled as aug-cc-pVDZ-PP.[24] To facilitate the description of the basis sets used in our calculations, aug-cc-pVDZ-PP[6-31G(d)] is used to represent the combination of the two different basis sets. For the optimization process, we first used the LanL2DZ basis set[25] with a relativistic pseudopotential for all of the atoms to obtain the equilibrium structures of the clusters, and then the geometries with real frequencies were used as starting configurations for reoptimization using the aug-cc-pVDZ-PP[6-31G(d)] basis sets. As has been pointed out,[26] "[because] aromaticity is not a directly measurable quantity, its magnitude is now generally evaluated in terms of structural, energetic, and magnetic criteria. However, magnetic properties are the most closely related to aromaticity." The nucleus-independent chemical shift (NICS) proposed by Schleyer et al.[13] is based on magnetic shieldings of a system. NICSs are widely used to characterize aromaticity and antiaromaticity, not only of cyclic molecular systems, but also of transition metal complexes, three-dimensional clusters, etc.[15] The analyses of the individual canonical molecular contributions to NICSs[27,28] (CMO−NICS) were carried out within the NBO 5.0 program.[27]

3. Results and Discussions

3.1. Pure Sn_{12}^{q-} and Pb_{12}^{q-} Clusters (q = 1 and 2). *3.1.1 Geometries and Stabilities.* As shown in Figure 1, the most stable geometries of Sn_{12}^{2-} (Pb_{12}^{2-}) clusters exhibit icosahedral (I_h) symmetries, while the structures of Sn_{12}^- (Pb_{12}^-) clusters

* To whom correspondence should be addressed. E-mail: tianwq@jlu.edu.cn.

† State Key Laboratory of Theoretical and Computational Chemistry, Institute of Theoretical Chemistry.

‡ College of Chemistry.

10.1021/jp073646n CCC: $37.00
Published on Web 07/31/2007

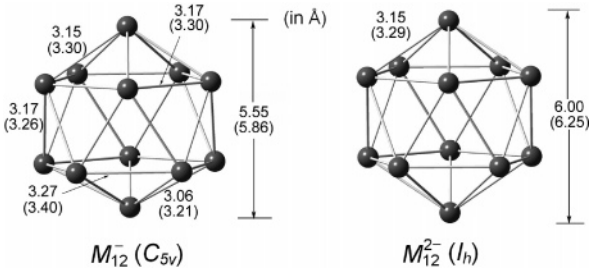

Figure 1. Optimized structures of M_{12}^- and M_{12}^{2-} (M = Sn and Pb). The bond distances and cage diameters are given in angstroms, and the values in parentheses are for the Pb clusters.

TABLE 1: HOMO−LUMO (H−L) Gaps and NICS Values at the Cage Center of M_{12}^- and M_{12}^{2-} (M = Sn and Pb), as Well as Vertical Detachment Energies (VDEs) of M_{12}^- [a]

	H−L gap (eV)	NICS (ppm)	VDE[b] (eV) theory	VDE[b] (eV) expt
Sn_{12}^-	1.30	2.0	3.25	3.34
Sn_{12}^{2-}	2.77	−5.0		
Pb_{12}^-	1.15	−8.0	3.03	3.14
Pb_{12}^{2-}	2.78	−20.7		
KSn_{12}	2.41	0.3		
KSn_{12}^-	2.02	−5.4	3.15	3.08
K_2Sn_{12}	2.47	−5.8		
KPb_{12}	1.85	−		
KPb_{12}^-	1.85	−	2.76	2.77
K_2Pb_{12}	2.23	−20.5		

[a] Data were obtained at the B3LYP/aug-cc-pVDZ-PP level. [b] Experimental values of VDEs were obtained from refs 16 and 29.

have slightly lower C_{5v} symmetry because of Jahn−Teller distortion. Sn_{12}^{2-} and Pb_{12}^{2-} have been studied both experimentally[8,16,29] and theoretically[8,10,16,29] in detail. In the present study, we perform comparisons of the electronic structures of Sn_{12}^-, Pb_{12}^-, Sn_{12}^{2-}, and Pb_{12}^{2-}. The detailed bond lengths of M_{12}^- and M_{12}^{2-} clusters (M = Sn and Pb) are presented in Figure 1. According to B3LYP/aug-cc-pVDZ(−PP) predictions, the diameters of Sn_{12}^{2-} and Pb_{12}^{2-} are 6.00 and 6.25 Å, respectively. However, the diameter of Sn_{12}^- (Pb_{12}^-) cluster is 5.55 (5.86) Å, shorter than that of Sn_{12}^{2-} (Pb_{12}^{2-}) by about 0.45 (0.39) Å, which is mainly caused by the depression of one apex atom. Compared to the Sn−Sn (Pb−Pb) bond lengths of 3.15 (3.29) Å within Sn_{12}^{2-} (Pb_{12}^{2-}), the bond lengths within Sn_{12}^- (Pb_{12}^-) vary slightly, with a deviation of less than 0.12 (0.11) Å. As listed in Table 1, the predicted first vertical detachment energy (VDE) value of C_{5v} Sn_{12}^-(Pb_{12}^-) is 3.25 (3.03) eV, in good agreement with the experimental value[16,29] of 3.34 (3.14) eV. Note that the VDE values were calculated as the energy differences between the neutrals and anions at the anion geometries. Compared to the large energy gap between the highest occupied molecular orbtial and the lowest unoccupied molecular orbital [HOMO−LUMO gap, 2.77 (2.78) eV] for dianionic Sn_{12}^{2-} (Pb_{12}^{2-}), the (α) HOMO−LUMO gap of 1.30 (1.15) eV for monoanionic Sn_{12}^- (Pb_{12}^-) is much smaller. Moreover, the predicted NICS value at the center of monoanionic Sn_{12}^- (Pb_{12}^-) cage is much less negative than that of dianionic Sn_{12}^{2-} (Pb_{12}^{2-}), as reported in Table 1. Although C_{5v} Pb_{12}^- exhibits aromatic character, the NICS value (−8.0 ppm) is much less negative than that of the Pb_{12}^{2-} cage (−20.7 ppm), suggesting that the addition of one electron to Pb_{12}^- greatly enhances its aromaticity. In addition, C_{5v} Sn_{12}^- and I_h Sn_{12}^{2-} exhibit NICS values of 2.0 and −5.0 ppm, respectively, indicating that Sn_{12}^- is nonaromatic and Sn_{12}^{2-} is slightly aromatic. Very recently, Chen et al. proposed[8] that two main factors can be assumed to determine the stability of a spherical

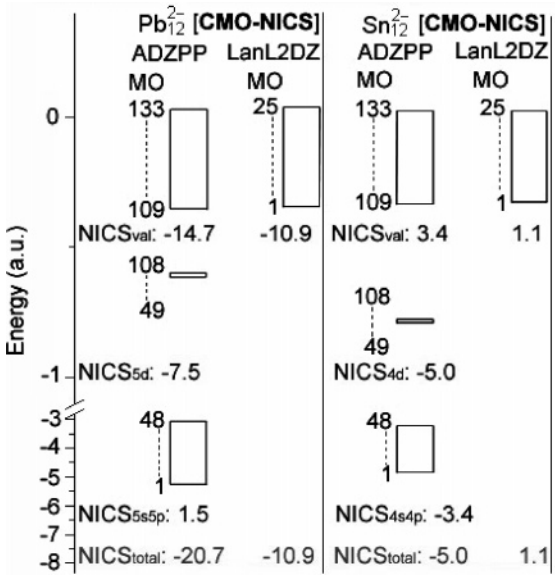

Figure 2. NICS contributions of 4s4p (5s5p) orbitals [$NICS_{4s4p}$ ($NICS_{5s5p}$)], 4d (5d) orbitals [$NICS_{4d}$ ($NICS_{5d}$)], and 5s5p (6s6p) orbitals [$NICS_{5s5p}$ ($NICS_{6s6p}$), i.e., $NICS_{val}$] to the total NICS ($NICS_{total}$) value of the Sn_{12}^{2-} (Pb_{12}^{2-}) cluster based on B3LYP/aug-cc-pVDZ-PP predictions, as well as $NICS_{val}$ (i.e., $NICS_{total}$) value based on the B3LYP/LanL2DZ predictions. ADZPP represents aug-cc-pVDZ-PP basis set, and the NICS values are in parts per million.

cluster, namely, aromatic stabilization and close packing. According to this principle, both the highly symmetrical close packing of I_h Sn_{12}^{2-} (Pb_{12}^{2-}) and the aromatic character contribute to its high stability. The observation[8] of $AlSn_{12}^+$ ($AlPb_{12}^+$) at high abundance in the mass spectrum confirms the stability of Sn_{12}^{2-} (Pb_{12}^{2-}); however, the lack of a direct observation of $AlSi_{12}^+$ or $AlGe_{12}^+$ in the spectrum might be related to the antiaromatic character of Si_{12}^{2-} and Ge_{12}^{2-}. Obviously, Wade's $2n + 2$ skeletal electron rule[30,31] is not adequate to predict the stabilities of "Zintl ions". E_n^{2-} (E = Si, Ge, Sn, Pb) bare main group element clusters (e.g., Zintl ions)[32] are known to exhibit structures similar to those of the well-known deltahedral boranes $B_nH_n^{2-}$ which follow Wade's rule with strong aromaticity. Unlike Sn_{12}^{2-} and Pb_{12}^{2-}, their the lighter congeners Ge_{12}^{2-} and Si_{12}^{2-} exhibit antiaromaticity,[33] although all of these clusters satisfy Wade's rule. Hence, analyses of aromaticity are necessary and helpful when aiming to predict the stabilities of Zintl ions.

3.1.2. Analyses of CMO−NICS. It should be mentioned that, in Chen et al.'s work,[8] the NICS value at the center of the Sn_{12}^{2-} cage was predicted to be 2.5 ppm at the GIAO (gauge-including atomic orbital)[34,35]-B3LYP/LanL2DZdp level of theory, which is qualitatively different from the value (−5.0 ppm) in our calculations. In the following section, we consider the source of this difference. The CMO−NICS analyses of Sn_{12}^{2-} and Pb_{12}^{2-} were performed based on GIAO-B3LYP/aug-cc-pVDZ-PP and GIAO-B3LYP/LanL2DZ, respectively. There are 133 and 25 occupied molecular orbitals for Sn_{12}^{2-} and Pb_{12}^{2-} based on the aug-cc-pVDZ-PP and LanL2DZ basis sets, respectively. The symmetry and NICS value of each molecular orbital for Sn_{12}^{2-} and Pb_{12}^{2-} based on B3LYP/aug-cc-pVDZ-PP are presented in Tables S1 and S2 (Supporting Information). From the analyses of natural bond orbital (NBO),[36,37] we conclude that MO(1)−MO(48), MO(49)−MO(108), and MO(109)−MO(133) of Sn_{12}^{2-} (Pb_{12}^{2-}) are mainly composed of 4s4p (5s5p), 4d (5d), and 5s5p (6s6p) electrons, respectively, at the B3LYP/aug-cc-pVDZ-PP level. As shown in Figure 2, the NICS contributions to the valence orbitals ($NICS_{val}$), 4d (5d) orbitals

[$NICS_{4d}$ ($NICS_{5d}$)], and 4s4p (5s5p) orbitals [$NICS_{4s4p}$ ($NICS_{5s5p}$)] for Sn_{12}^{2-} (Pb_{12}^{2-}) based on GIAO-B3LYP/aug-cc-pVDZ-PP, as well as $NICS_{val}$ for Sn_{12}^{2-} (Pb_{12}^{2-}) based on GIAO-B3LYP/LanL2DZ are presented. $NICS_{val}$ of Sn_{12}^{2-} (Pb_{12}^{2-}) obtained with GIAO-B3LYP/aug-cc-pVDZ-PP is very close to that of Sn_{12}^{2-} (Pb_{12}^{2-}) obtained with GIAO-B3LYPL/LanL2DZ, i.e., 3.4 (−14.7) vs 1.1 (−10.9) ppm. The NICS contributions from 4s4p (5s5p) orbitals are small, being −3.4 (1.5) ppm for Sn_{12}^{2-} (Pb_{12}^{2-}). However, $NICS_{4d}$ and $NICS_{5d}$ are −5.0 and −7.5 ppm, respectively, for Sn_{12}^{2-} and Pb_{12}^{2-}. The $NICS_{5d}$ value (−7.5 ppm) of Pb_{12}^{2-} is a main contribution to $NICS_{total}$ (−20.7 ppm), and the $NICS_{4d}$ value of Sn_{12}^{2-} significantly influences the aromatic character of the cage. In conclusion, the inner d orbitals strongly contribute to the total NICS values in both the Sn_{12}^{2-} and Pb_{12}^{2-} clusters. However, d-orbital aromaticity was found to exist only in transition-metal-based clusters in previous works.[17−20] Our predictions provide the first quantitative evidence for the existence of d-orbital aromaticity in group IV metal-based clusters. In particular, the d orbitals of Sn and Pb atoms are usually viewed as semicore orbitals, unlike the d orbitals of transition metals, which are in the valence region.

To confirm that the small-core pseudopotential (PP) basis set is accurate enough to predict the NICS values of the Sn and Pb clusters, i.e., the core has nearly no contribution to the total NICS, we also performed CMO−NICS analyses on Sn_{12}^{2-} with GIAO-B3LYP/3-21G(d)//B3LYP/aug-cc-pVDZ-PP. We note that this basis set should give a qualitative description of the detailed NICS contribution of the molecular orbitals (especially for inner orbitals). Indeed, the calculations showed that the NICS contribution of the core ($NICS_{core}$) is −0.1 ppm and $NICS_{4d}$ is −5.7 ppm, clearly reflecting that the core makes nearly no contribution to the total NICS and that $NICS_{4d}$ is very close to the value obtained with B3LYP/aug-cc-pVDZ-PP. The detailed NICS contributions of each molecular orbital for Sn_{12}^{2-} based on GIAO-B3LYP/3-21G(d)//B3LYP/-aug-cc-pVDZ-PP are reported in Table S3 (Supporting Information).

For systems containing heavy elements, recent investigations[18,38] show that the NICS values based on large-core PPs (LanL2DZ) remain reliable when predicting properties that depend mostly on the regions outside the core. However, the present results suggest that the large-core PP basis set LanL2DZ does not allow for clear aromaticity scale delineation for Sn- (and Pb-) containing clusters, because the d orbitals are not included in the valence shell and the d orbitals contribute to the total NICS values of the M_{12}^{2-} clusters. For this reason, it is recommended that the d orbitals should be taken into account explicitly if the aim is to obtain more accurate predictions of the degree of aromaticity for Sn- (or Pb-) containing compounds. We expect that these NICS predictions in our study will inspire more efforts in studying the d-orbital aromaticity of main-group-metal-based clusters.

3.2. Aromatic Characters and Stabilities of KM_{12}, KM_{12}^-, and K_2M_{12} Clusters (M = Sn and Pb). Cui et al.[16,29] successfully observed stable anionic KM_{12}^- during photoelectron spectroscopy experiments. Herein, we not only analyze the aromatic character of the characterized anionic KM_{12}^- but also discuss the aromatic character of neutral KM_{12} and K_2M_{12}. The geometries of the most stable isomers for the neutral KM_{12}, anionic KM_{12}^-, and neutral K_2M_{12} clusters (M = Sn and Pb) are presented in Figure S1 (Supporting Information). For neutral KM_{12}, a distorted icosahedral M_{12} with a capping K atom outside of the cage (labeled A1 in Figure S1) is the most stable isomer with C_s symmetry. For anionic KM_{12}^-, the geometry of the most stable isomer (B1) is similar to that of neutral KM_{12}; however, KM_{12}^- presents a higher symmetry (C_{3v}). Further investigation of the most stable structure KM_{12}^- shows that its M_{12}^{2-} moiety is very similar to the pure icosahedral M_{12}^{2-} discussed above. In addition, the four most stable isomers (C1−C4) of neutral K_2Sn_{12} (K_2Pb_{12}), all of which retain a slightly distorted icosahedral cage, lie within an energy range of only 0.16 (0.12) eV.

The calculated NICS values of K-coordinated Sn (Pb) clusters are very similar to those of the isoelectronic pure Sn (Pb) clusters, as shown in Table 1. For example, the NICS value at the cage center of KSn_{12}^- is −5.4 ppm, very close to −5.0 ppm of Sn_{12}^{2-}. As expect, further CMO−NICS analyses of KSn_{12}^- show that the d-orbital contribution ($NICS_{4d}$) is −5.2 ppm, nearly the same as that of Sn_{12}^{2-} (−5.0 ppm), suggesting that the d-orbital contribution is retained in the K-coordinated clusters. Moreover, the molecular orbital analyses of KSn_{12}^- (KPb_{12}^-) show that there are eight π electrons occupying four π orbitals, which clearly reflects the closed-shell nature of the π subsystem, according to Hirsh's $2(N+1)^2$ rule.[39] Note that the molecular orbitals of KSn_{12}^- are very similar to those of KPb_{12}^-, and the molecular orbitals of KPb_{12}^- are provided in Figure S2 (Supporting Information). The case for neutral K_2Sn_{12} (K_2Pb_{12}) is similar to that for anionic KSn_{12}^- (KPb_{12}^-). In summary, the closed-shell nature of the π subsystem together with the aromatic character of both KM_{12}^- and K_2M_{12} (M = Sn and Pb) enable them to exist as stable clusters.

4. Conclusions

The density-functional-theory-based B3LYP method with the aug-cc-pVDZ-PP[6-31G(d)] basis sets has been employed to study monoanionic M_{12}^- and dianionic M_{12}^{2-}, as well as KM_{12}, KM_{12}^-, and K_2M_{12} (where M = Sn and Pb). The NICS values at the cage center of Sn_{12}^{2-} and Pb_{12}^{2-} are −5.0 and −20.7 ppm, respectively, implying their aromatic character. Further CMO−NICS analyses show that the $NICS_{4d}$ (Sn_{12}^{2-}) and $NICS_{5d}$ (Pb_{12}^{2-}) values are −5.0 and −7.5 ppm, respectively, which contribute significantly to the total NICS value. This provides the first quantitative evidence for the existence of d-orbital aromaticity in Sn- and Pb-based clusters with three-dimensional structures. Unlike the d orbitals of transition metals in the valence region, the d orbitals of Sn and Pb are fully occupied and viewed as semicore orbitals. We expect that the present study will inspire more efforts to study d-orbital aromaticity in main-group-metal-based clusters. According to the NICS predictions from LanL2DZ and aug-cc-pVDZ-PP[6-31G(d)], larger basis sets are indispensable for obtaining accurate predictions of the aromaticity of Sn- and Pb-based clusters because they include the d orbitals. Investigations show that the aromatic characters of KM_{12}, KM_{12}^-, and K_2M_{12} clusters are retained, i.e., their NICS values are very close to those of the isoelectronic M_{12}^- or M_{12}^{2-} clusters. The d-orbital NICS contributions within K-coordinated clusters (KM_{12}^- and K_2M_{12}) are nearly the same as the d-orbital NICS contributions of the pure M_{12}^{2-} clusters.

Acknowledgment. W.Q.T. acknowledges the startup funds from Jilin University. This work was supported by the Chinese Natural Science Foundation under Grant 20473031.

Supporting Information Available: Each MO contribution to the total NICS value of M_{12}^{2-} (M = Sn and Pb); predicted isomers of KM_{12}, KM_{12}^-, and K_2M_{12} clusters; and representations of the frontier molecular orbitals of KPb_{12}^-. This material is available free of charge via the Internet at http://pubs.acs.org.

References and Notes

(1) Zhang, X.; Tang, Z.; Gao, Z. *Rapid Comm. Mass Spectrom.* **2003**, *17*, 621.
(2) Neukermans, S.; Janssens, E.; Chen, Z.; Silverans, R. E.; Schleyer, P. v. R.; Lievens, P. *Phys. Rev. Lett.* **2004**, *92*, 163401.
(3) Esenturk, E. N.; Fetteinger, J.; Lam, Y.-F.; Eichhorn, B. *Angew. Chem., Int. Ed.* **2004**, *43*, 2132.
(4) Fässler, T. F.; Hoffmann, S. D. *Angew. Chem., Int. Ed.* **2004**, *43*, 6242.
(5) Rajesh, C.; Majumder, C. *Chem. Phys. Lett.* **2006**, *430*, 101.
(6) Neukermans, S.; Wang, X.; Veldeman, N.; Janssens, E.; Silverans, R. E.; Lievens, P. *Int. J. Mass Spectrom.* **2006**, *252*, 145.
(7) Esenturk, E. N.; Fettinger, J.; Eichhorn, B. *J. Am. Chem. Soc.* **2006**, *128*, 9178.
(8) Chen, Z.; Neukermans, S.; Wang, X.; Janssens, E.; Zhou, Z.; Silverans, R. E.; King, R. B.; Schleyer, P. v. R.; Lievens, P. *J. Am. Chem. Soc.* **2006**, *128*, 12829.
(9) Dognon, J.-P.; Clavaguéra, C.; Pyykkö, P. *Angew. Chem., Int. Ed.* **2007**, *46*, 1427.
(10) Chen, D.-L.; Tian, W. Q.; Lu, W.-C.; Sun, C.-C. *J. Chem. Phys.* **2006**, *124*, 154313; **2006**, *125*, 049901 (E).
(11) Chen, D.-L.; Tian, W. Q.; Sun, C.-C. *Phys. Rev. A* **2007**, *75*, 013201.
(12) Schleyer, P. v. R.; Maerker, C.; Dransfeld, A.; Jiao, H.; Van Eikema Hommes, N. J. R. *J. Am. Chem. Soc.* **1996**, *118*, 6317.
(13) Boldyrev, A. I.; Wang, L.-S. *Chem. Rev.* **2005**, *105*, 3716.
(14) Chen, Z.; Wannere, C. S.; Corminboeuf, C.; Puchta, R.; Schleyer, P. v. R. *Chem. Rev.* **2005**, *105*, 3842.
(15) Cui, L.-F.; Huang, X.; Wang, L.-M.; Li, J.; Wang, L.-S. *Angew. Chem., Int. Ed.* **2007**, *46*, 742.
(16) Cui, L.-F.; Huang, X.; Wang, L.-M.; Zubarev, D. Y.; Boldyrev, A. I.; Li, J.; Wang, L.-S. *J. Am. Chem. Soc.* **2006**, *128*, 8390.
(17) Wannere, C. S.; Corminboeuf, C.; Wang, Z.-X.; Wodrich, M. D.; King, R. B.; Schleyer, P. v. R. *J. Am. Chem. Soc.* **2005**, *127*, 5701.
(18) Corminboeuf, C.; Wannere, C. S.; Roy, D.; King, R. B.; Schleyer, P. v. R. *Inorg. Chem.* **2006**, *45*, 214.
(19) Huang, X.; Zhai, H.-J.; Kiran, B.; Wang, L.-S. *Angew. Chem., Int. Ed.* **2005**, *44*, 7251.
(20) Huang, X.; Zhai, H.-J.; Waters, T.; Li, J.; Wang, L.-S. *Angew. Chem., Int. Ed.* **2006**, *45*, 657.
(21) Becke, A. D. *J. Chem. Phys.* **1993**, *98*, 5648.
(22) Lee, C.; Yang, W.; Parr, P. G. *Phys. Rev. B* **1993**, *37*, 785.
(23) Frisch, M. J.; Trucks, G. W.; Schlegel, H. B.; Scuseria, G. E.; Robb, M. A.; Cheeseman, J. R.; Zakrzewski, V. G.; Montgomery, J. A., Jr.; Stratmann, R. E.; Burant, J. C.; Dapprich, S.; Millam, J. M.; Daniels, A. D.; Kudin, K. N.; Strain, M. C.; Farkas, O.; Tomasi, J.; Barone, V.; Cossi, M.; Cammi, R.; Mennucci, B.; Pomelli, C.; Adamo, C.; Clifford, S.; Ochterski, J.; Petersson, G. A.; Ayala, P. Y.; Cui, Q.; Morokuma, K.; Malick, D. K.; Rabuck, A. D.; Raghavachari, K.; Foresman, J. B.; ioslowski, J.; Ortiz, J. V.; Stefanov, B. B.; Liu, G.; Liashenko, A.; Piskorz, P.; Komaromi, I.; Gomperts, R.; Martin, R. L.; Fox, D. J.; Keith, T.; Al-Laham, M. A.; Peng, C. Y.; Nanayakkara, A.; Gonzalez, C.; Challacombe, M.; Gill, P. M. W.; Johnson, B. G.; Chen, W.; Wong, M. W.; Andres, J. L.; Head-Gordon, M.; Replogle, E. S.; Pople, J. A. *Gaussian 03*, revision C.02; Gaussian, Inc.: Pittsburgh, PA, 2004.
(24) Peterson, K. A. *J. Chem. Phys.* **2003**, *119*, 11099.
(25) Wadt, W. R.; Hay, P. J. *J. Chem. Phys.* **1985**, *82*, 299.
(26) Fallah-Bagher-Shaidaei, H.; Wannere, C. S.; Corminboeuf, C.; Puchta, R.; Schleyer, P. v. R. *Org. Lett.* **2006**, *8*, 863.
(27) Bohmann, J. A.; Winhold, F.; Farrar, T. C. *J. Chem. Phys.* **1997**, *107*, 1173.
(28) Heine, T.; Schleyer, P. v. R.; Corminboeuf, C.; Seifert, G.; Reviakine, R.; Weber, J. *J. Phys. Chem. A* **2003**, *107*, 6470.
(29) Cui, L.-F.; Huang, X.; Wang, L.-M.; Li, J.; Wang, L.-S. *J. Phys. Chem. A* **2006**, *110*, 10169.
(30) Wade, K. *Chem. Commun.* **1971**, 792.
(31) Wade, K. *Adv. Inorg. Chem. Radiochem.* **1976**, *18*, 1.
(32) Fässler, T. F. *Coord. Chem. Rev.* **2001**, *215*, 347.
(33) King, R. B.; Heine, T.; Corminboeuf, C.; Schleyer, P. v. R. *J. Am. Chem. Soc.* **2004**, *126*, 430.
(34) Schreckenbash, G.; Ziegler, T. *J. Phys. Chem.* **1995**, *99*, 606.
(35) Cheeseman, J. R.; Trucks, G. W.; Keith, T. A.; Frisch, M. *J. Chem. Phys.* **1996**, *104*, 5497.
(36) Carpenter, J. E.; Weinhold, F. *J. Mol. Struct. (THEOCHEM)* **1988**, *169*, 41.
(37) Reed, A. E.; Curtiss, L. A.; Weinhold, F. *Chem. Rev.* **1988**, *88*, 899.
(38) Corminboeuf, C. *Chem. Phys. Lett.* **2006**, *437*, 441.
(39) Hirsch, A.; Chen, Z.; Jiao, H. *Angew. Chem., Int. Ed.* **2000**, *39*, 3915; **2001**, *40*, 2834.